Websites:
http://www.jofamericanscience.org
http://www.sciencepub.net

Emails:
editor@sciencepub.net
sciencepub@gmail.com

MARSLAND PRESS
Multidisciplinary Academic Journal Publisher

# Thermal-structural behavior of axially loaded CFST in fire condition

A.T. Kassem

Assistant Professor, Civil Engineering Department, Faculty of engineering / Beni-Suef University, Egypt
Abdelraouf_kassem@yahoo.com

**Abstract:** This paper aims to investigate both thermal and structural behavior of **C**oncrete **F**illed **S**teel **T**ubes when subjected to a fire load, in order to figure out roles of various structural parameters on CFST fire endurance. Two main fire scenarios have been considered, by applying fire load at full column circumference or at half the circumference only. The ISO 834 fire curve has been considered as a standard fire load. Ansys has been used as a numerical modelling tool, where verification of both thermal and structural outputs has been performed using data, available in the literature. Buckling has been considered as the main structural failure criterion. Various structural parameters have been considered to investigate their role regarding column fire endurance. Column overall diameter, tube thickness, overall stiffness, and steel ratio have been considered as structural parameters. A parametric study has been conducted for both fire scenarios and structural parameters. Significance of various parameters to the research point has been clarified and presented in the paper.

[A.T. Kassem. **Thermal-structural behavior of axially loaded CFST in fire condition**. J Am Sci 2019;15(4):101-112]. ISSN 1545-1003 (print); ISSN 2375-7264 (online). http://www.jofamericanscience.org. 13. doi:10.7537/marsjas150219.13.

**Key words**
CFST, failure, buckling, fire, ISO 834

## 1. Introduction

Fire effects on steel structures are catastrophic, while in case of concrete structures are mild. Composite structures represent a challenge in understanding their behavior. Sometimes composite behavior is intermediate between concrete and steel, other cases the rigid connection between steel and concrete, in conjunction with difference in thermal response, increases thermally induced internal stresses; and consequently, composite structures behave in a special way.

CFST are used extensively in high rise buildings, to minimize column's cross sections. Passive structural fire engineering aims to ensure a building can sustain fire load for a specific time period, to ensure the ability of resident's evacuation. Preventing a building from collapse requires ensuring stability of main structural elements, especially columns. The case of CFST represents a special behavior. Steel tube represents the outer cover of the column, subjected to highest thermal load and most vulnerable to this effect. The high temperature of steel results in an increased expansion in steel tube than concrete core; and consequently, additional stresses are generated at the interface. Research work, related to CFST includes two main fields. The first is related to thermal response of CFST and aims to identify temperature distribution within the CFST as a function of time within the whole cross section. The second aims to study load carrying capacity, either during (as in this study) or post fire. Load carrying capacity is usually presented in the form of fire endurance for a specific load ratio.

A number of recent researches has been studied to identify research gap and parameters to study, precisely.

João Rodrigues & Luis Laim[1] studied the behavior of concrete filled columns subjected to fire. They introduced various cross-sectional shapes with a total number of fourteen specimens and evaluated formulae, presented in Eurocode; that has been proved to be in-satisfactory, in case of restrained columns. They concluded that stiffness is not a significant parameter for fire endurance of concrete columns.

Tiziano Perea et al[2] performed full-scale tests on slender concrete-filled tubes. They examined columns subjected to various loading protocols, including pure compression and combinations of compression and bending moments. Modelling showed an accepted correlation within the elastic range, but showed some difference for inelastic buckling.

Venkatish Kodur et al[3] Tiziano Perea et studied high temperature properties of steel for fire resistance modelling of structures. They compared experimental results with various models, available in the literature. They studied thermal properties, as specific heat and thermal conductivity. Moreover, they considered structural properties, as strength and modulus of elasticity. Other properties such as thermal creep have also been studied. They proposed some modification to ASCE thermal properties above 400ºc. Moreover, significant changes to thermal-structural properties have been introduced. They recommended the use of Eurocode stress-strain relations than ASCE ones.

J Khalaf, Z Huang, & Mizi Fan[4] used the software "Vulcan" to study the effect of bond between steel reinforcement and concrete under fire conditions. They considered reinforcement yielding stress, concrete characteristic strength and cover. They reached that the most significant factor affecting bond is concrete cover.

Lin-Hai Han, et al[5] studied the behavior of concrete encased concrete filled steel tubes, subjected to axial load; to identify the bond parameters between steel tube and concrete on both sides. They found that bond parameters on the steel tube outer face resulted in a higher bond than the inner face.

R. Imani et al[6] established a finite element simulation of concrete-filled double-skin tube columns subjected to post-earthquake fires, using Abaqus. They considered plastic behavior of columns in fire, concrete cracking, and cyclic loading behavior. The proposed model included the insertion of a tensile crack at the location of maximum tensile stresses. Comparisons between the proposed model and experimental investigations showed accepted correlation.

## 2. Finite element model

Dealing with the research problem required the preparation of a finite element model, to deal with both thermal and structural aspects of the problem. The thermal problem has been solved first to extract temperature distribution as a function of time through the column cross section. Resulting temperatures have been used to determine material degradation within the cross section, as a function of both time and temperature. Moreover, thermal induced stresses have also been considered. Structural modelling has been performed after thermal outputs extraction. Structural analysis considered both load induced stresses in the form of load ratio (ratio between the applied load and theoretical buckling load, free of thermal effects) and thermal induced stresses. Thermal fire load has been considered in two scenarios, representing the cases of full and half circumferential load, as shown in figure (1). The finite element model used solid elements, in a quadlateral meshing form, as shown in figure (2)

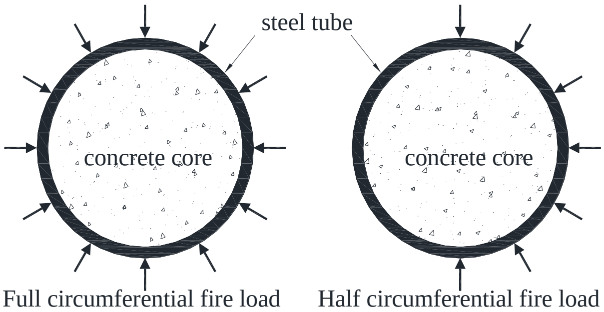


**Figure 1.** Problem fire load cases

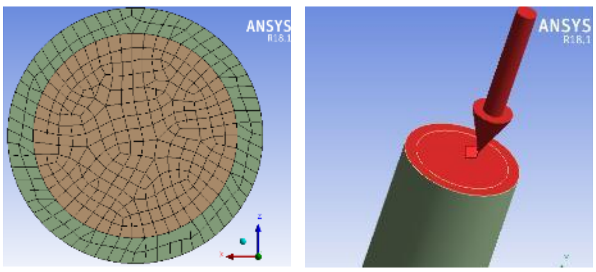


a) F.E. Mesh b) F.E. Axial Load

**Figure 2.** Finite Element Model

Material non-linearities for both thermal and structural analyses have been considered, in accordance with temperature dependent material properties; presented in Eurocode[7]. Figures (3) up to (7) summarize material degradation properties, implemented in the finite element model. While geometric non-linearity has been implemented through allowing the model to regenerate the stiffness matrix after each loads step, enabling large displacement analysis.

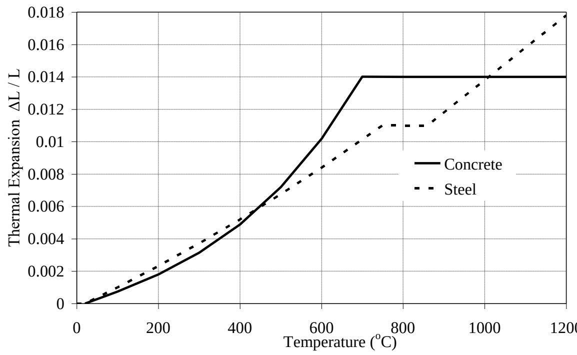


**Figure 3.** Thermal Expansion at Elevated Temperature [7]

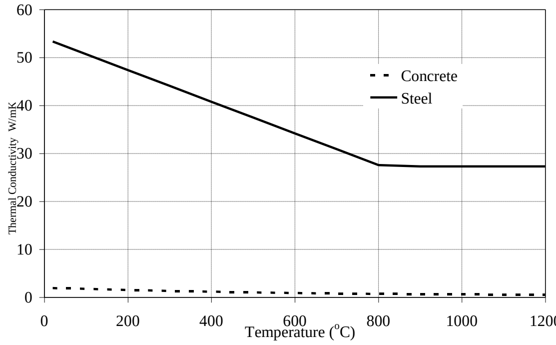


**Figure 4.** Thermal Conductivity at Elevated Temperature [7]

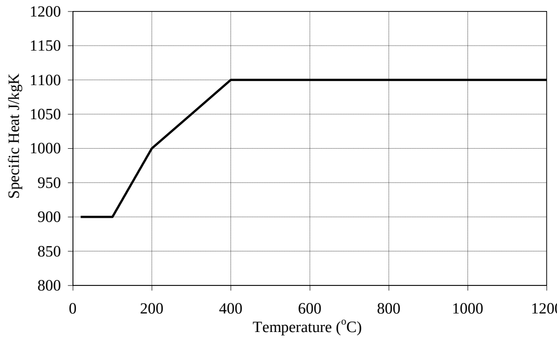


**Figure 5.** Concrete Specific Heat at Elevated Temperature [7]

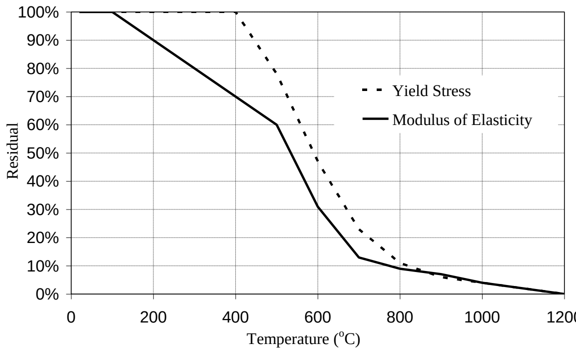


**Figure 6.** Steel structural properties at elevated temperature[7]

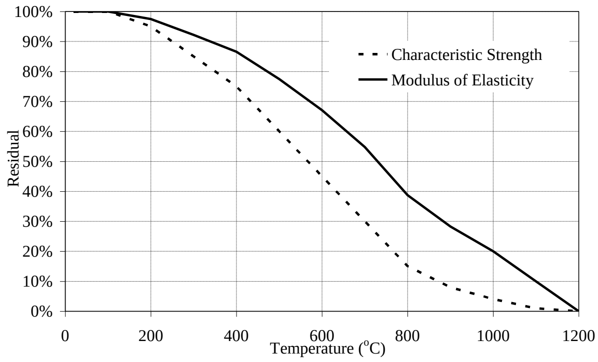


**Figure 7.** Concrete structural properties at elevated temperature [7]

Figure 8 shows model deformed and undeformed shapes. Various 3D mesh finenesses have been implemented for each model, to ensure reaching an accepted level of accuracy.

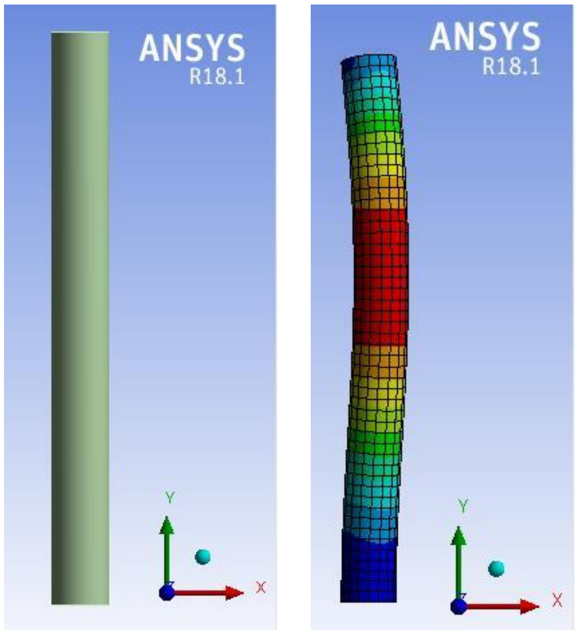


a) un-deformed shape B) deformed shape

**Figure 8.** Finite Element Model

The finite element model has been verified for both thermal and structural analyses. Thermal verification has been performed by comparing thermal outputs with data available in the literature, as shown in figures (9) up to (11), for CFST subjected to various thermal scenarios. Thermocouples have been installed at the surface, center and in between within the CFST. Modeling showed a good correlation with recorded temperatures. Other verification has been performed with temperature profiles, available in in the eurocode[7], for a column of diameter 300mm. An accepted level of correlation appeared with Eurocode, based on the application of ISO834 standard fire curve, as shown in figure (12).

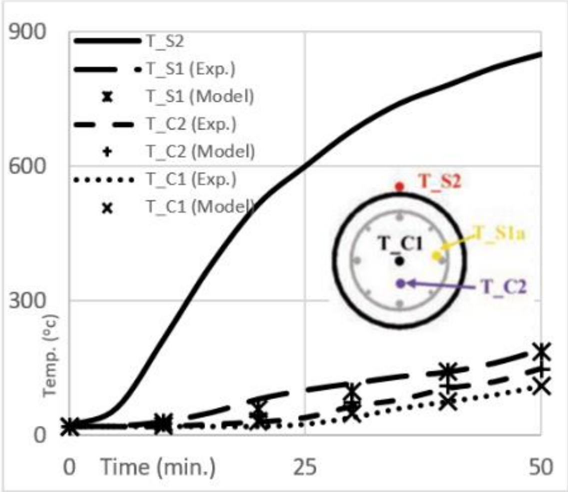


**Figure 9.** Verification of thermal model Laim[1]

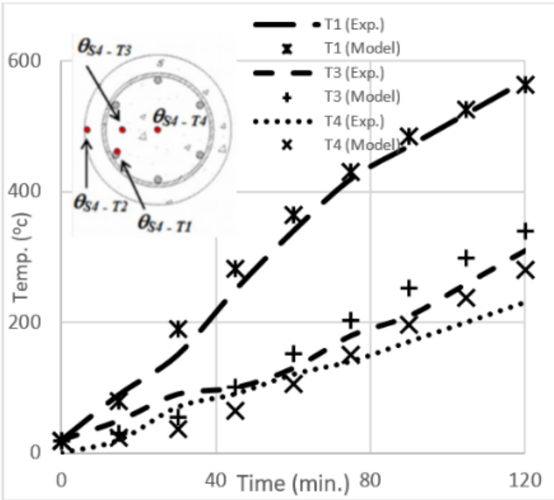


**Figure 10.** Verification of thermal model Korzen [11]

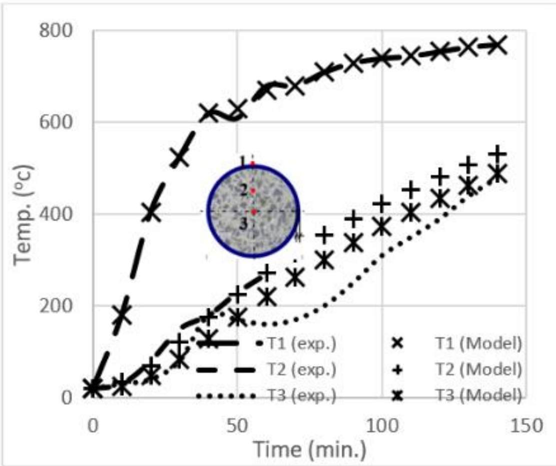


**Figure 11.** Verification of thermal model Ghannam[12]

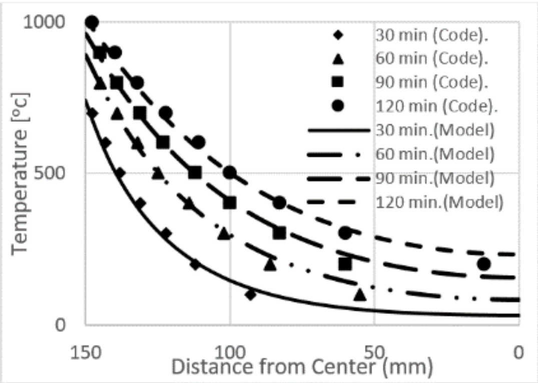


**Figure 12.** Verification of thermal model Eurocode[7]

After the model has been thermally verified. Outputs, in the form of temperature contours, as a function of time have been extracted for both the cases of full and half circumferential thermal load application. Figures (13) up to (16) show temperature distribution through columns sections after 60 and 240 minutes for full and half thermal loads.

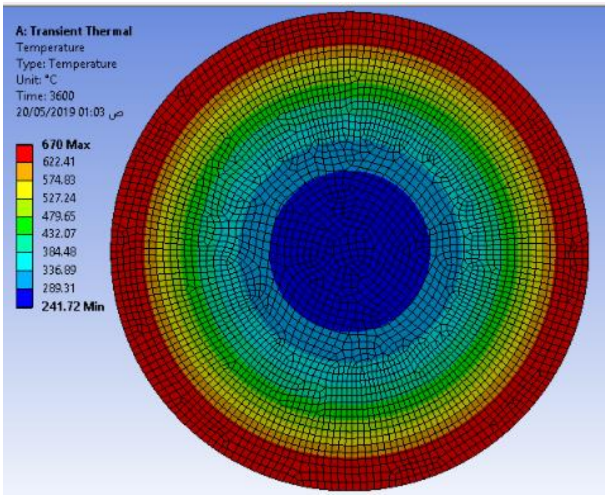


**Figure 13.** Temp. Contours for CFST Φ 200 mm t 10 mm after 60 min.

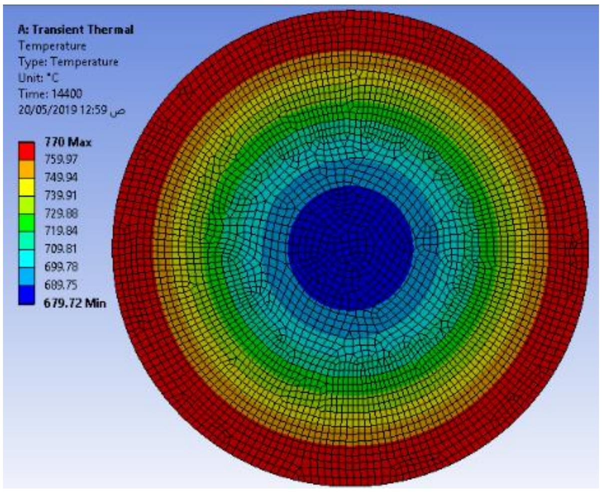


**Figure 14.** Temp. Contours for CFST Φ 200 mm t 10 mm after 240 min.

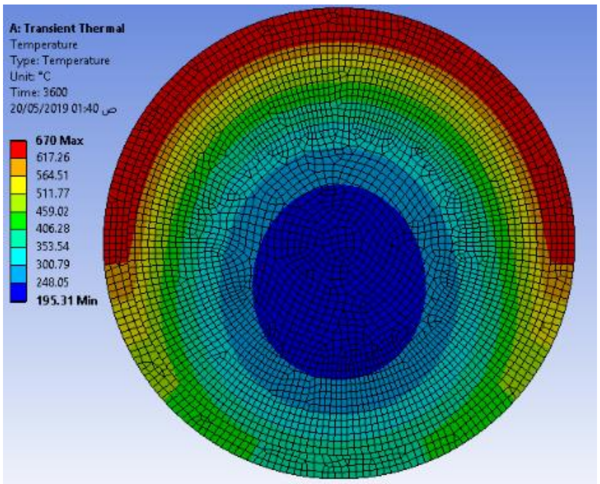


**Figure 15.** Temp. Contours for CFST Φ 200 mm t 10 mm after 60 min. (single sided thermal load)

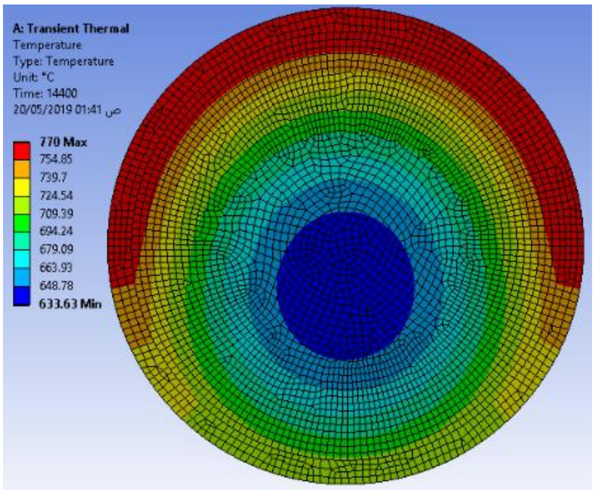


**Figure 16.** Temp. Contours for CFST Φ 200 mm t 10 mm after 240 min. (single sided thermal load)

Thermo-structural verification of the finite element model has been performed by comparing fire endurance generated from the model by that recorded experimentally by Rodrigues & Laim[1], for specific load ratios. Figure (17) presents the ratio of model to experimental fire endurance. It could be noticed that the model resulted in conservative values for fire endurance, mostly exceeding 90% of that recorded experimentally.

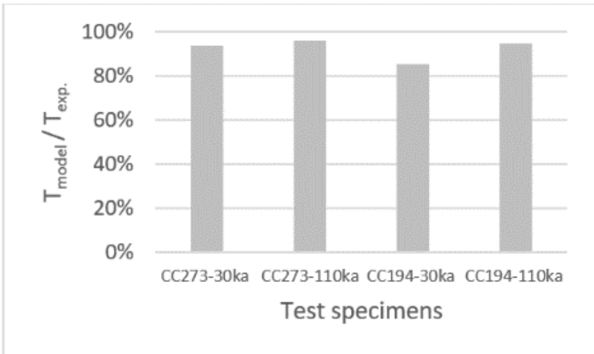


**Figure 17.** Thermo-structural verification of F.E. model

### 3. Parametric Study

After full verification of the finite element model, a parametric study has been prepared to clarify the role of various structural and geometric parameters on the behavior of CFST in fire condition. Table (1) shows geometric parameters of various models used in the parametric study, where Φ is column external diameter and t is tube thickness in millimeters. The parametric study aimed to consider the effects of overall stiffness, column diameter, exposure condition, tube thickness and steel ratio on fire endurance.

**Table 1.** Parametric Study Details

| Φ<br>T | 100 | 200 | 300 | 400 | 600 | 800 | 1600 |
|---|---|---|---|---|---|---|---|
| 10 | ■ | ■ |  | ■ | ■ | ■ | ■ |
| 20 | ■ | ■ |  | ■ | ■ | ■ | ■ |
| 30 |  |  | ■ | ■ |  |  |  |
| 40 |  | ■ |  | ■ | ■ | ■ |  |
| 60 |  |  |  |  | ■ |  |  |
| 80 |  |  |  | ■ |  | ■ | ■ |

The first phase of finite element analysis was the thermal analysis, to identify temperature distribution within the CFST sections. Figures (18) up to (39) present a brief interpretation of the analyzed models. Studying temperature distribution figures gives a clear vision of the thermal response of CFST.

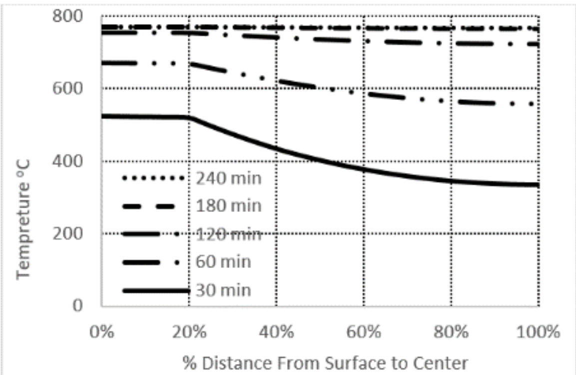


**Figure 18.** Temp. Dist. Through CFST Φ 100 mm t 10 mm

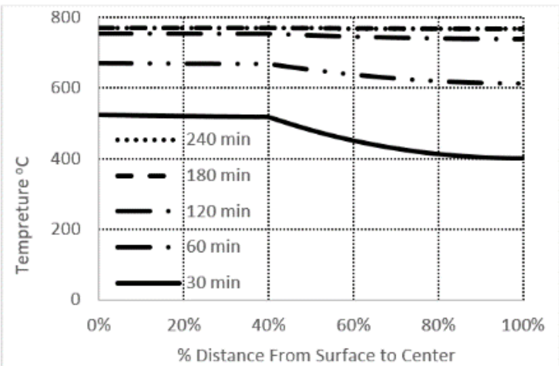


**Figure 19.** Temp. Dist. Through CFST Φ 100 mm t 20 mm

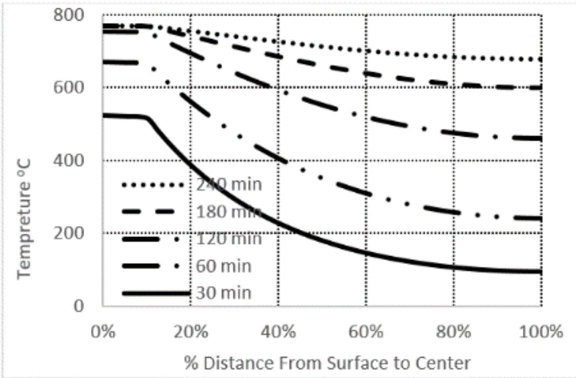


**Figure 20.** Temp. Dist. Through CFST Φ 200 mm t 10 mm

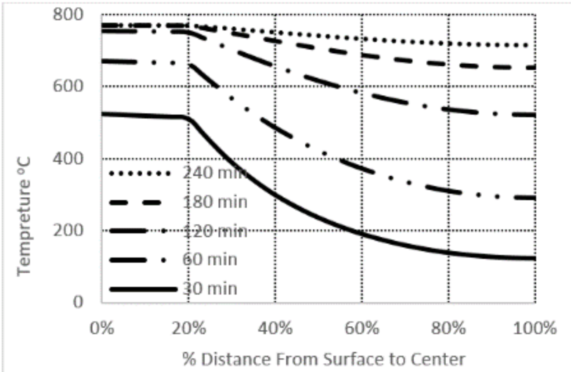


**Figure 21.** Temp. Dist. Through CFST Φ 200 mm t 20 mm

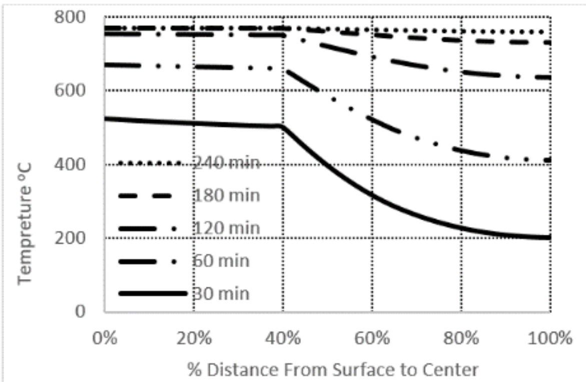


**Figure 22.** Temp. Dist. Through CFST Φ 200 mm t 40 mm

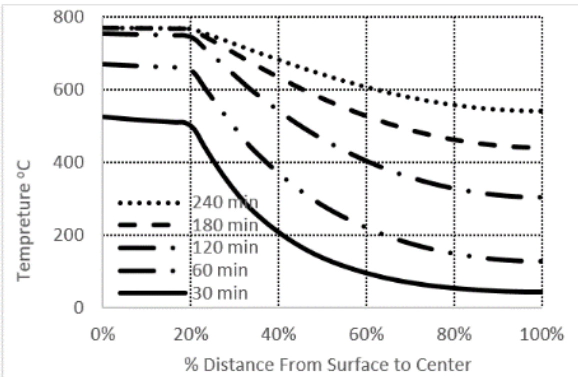


**Figure 23.** Temp. Dist. Through CFST Φ 300 mm t 30 mm

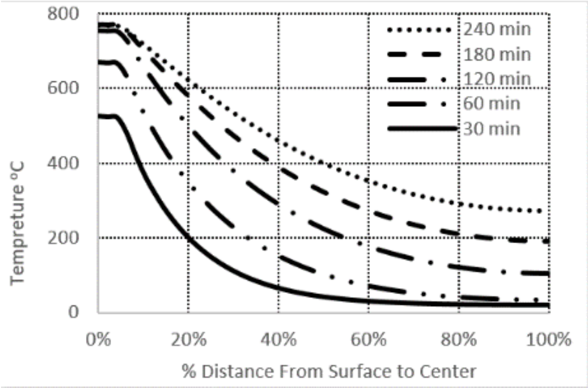


**Figure 24.** Temp. Dist. Through CFST Φ 400 mm t 10 mm

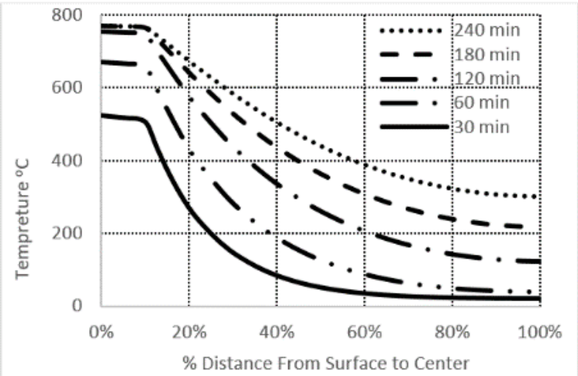


**Figure 25.** Temp. Dist. Through CFST Φ 400 mm t 20 mm

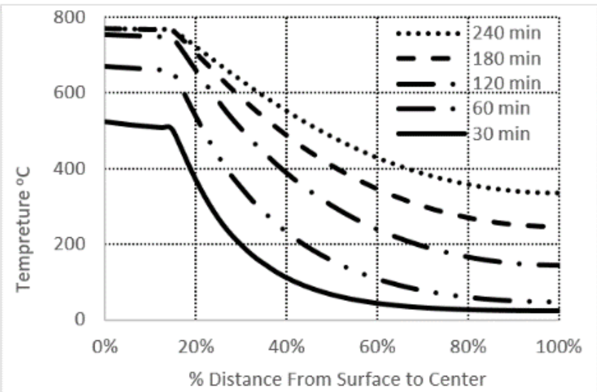


**Figure 26.** Temp. Dist. Through CFST Φ 400 mm t 30 mm

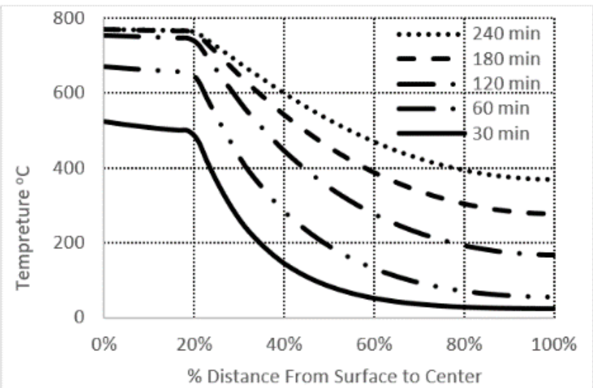


**Figure 27.** Temp. Dist. Through CFST Φ 400 mm t 40 mm

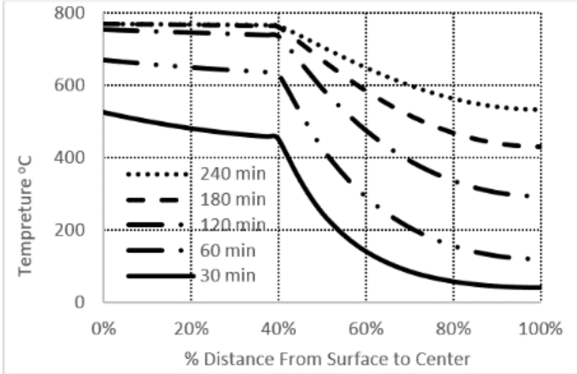


**Figure 28.** Temp. Dist. Through CFST Φ 400 mm t 80 mm

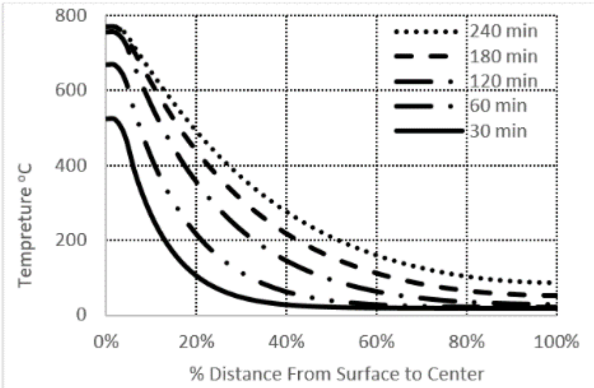


**Figure 29.** Temp. Dist. Through CFST Φ 600 mm t 10 mm

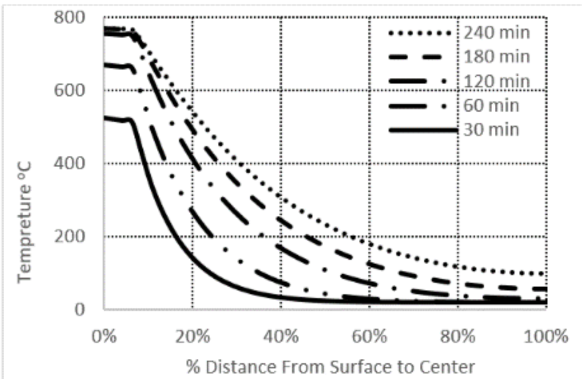


**Figure 30.** Temp. Dist. Through CFST Φ 600 mm t 20 mm

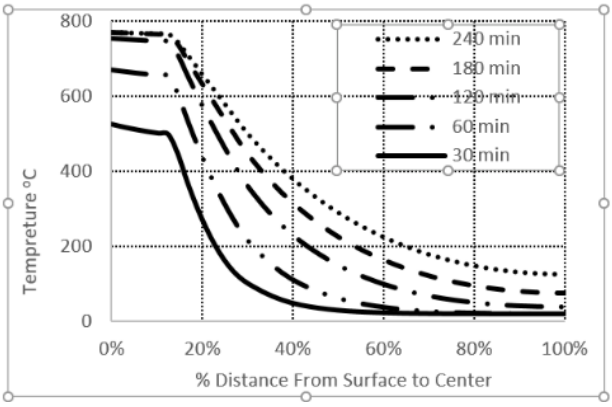


**Figure 31.** Temp. Dist. Through CFST Φ 600 mm t 40 mm

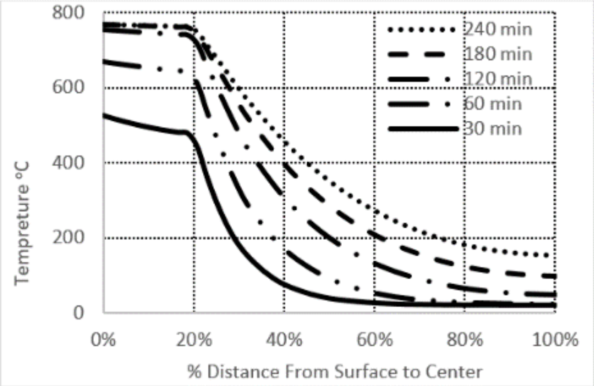


**Figure 32.** Temp. Dist. Through CFST Φ 600 mm t 60 mm

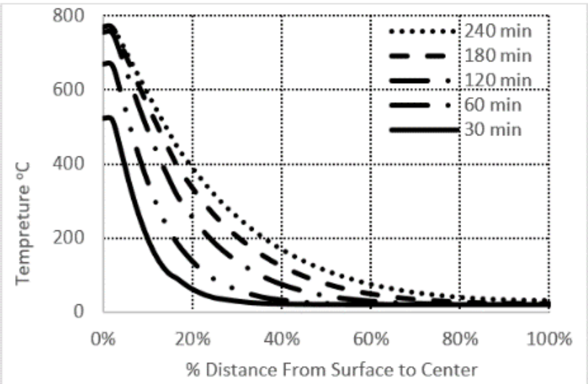


**Figure 33.** Temp. Dist. Through CFST Φ 800 mm t 10 mm

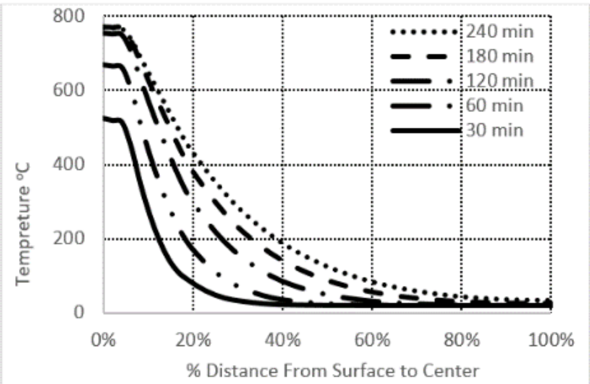


**Figure 34.** Temp. Dist. Through CFST Φ 800 mm t 20 mm

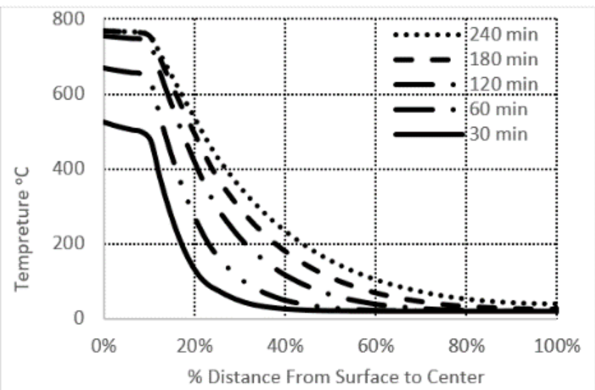


**Figure 35.** Temp. Dist. Through CFST Φ 800 mm t 40 mm

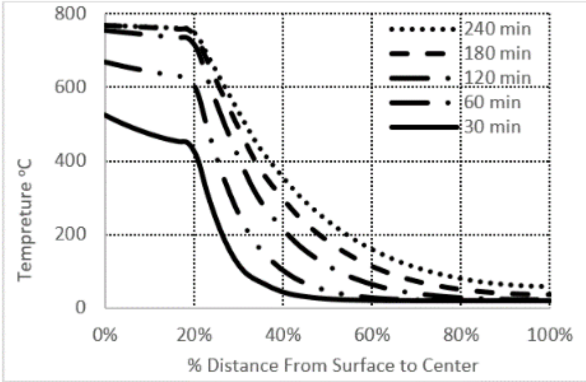


**Figure 36.** Temp. Dist. Through CFST Φ 800 mm t 80 mm

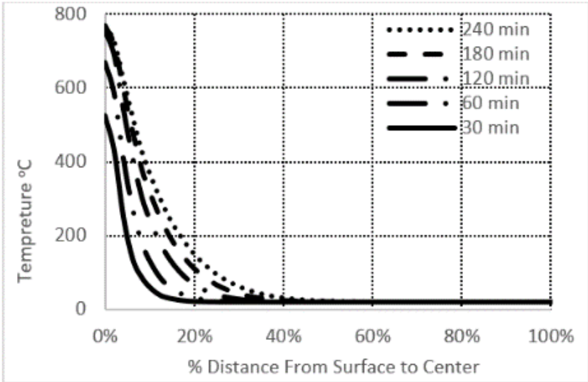


**Figure 37.** Temp. Dist. Through CFST Φ 1600 mm t 10 mm

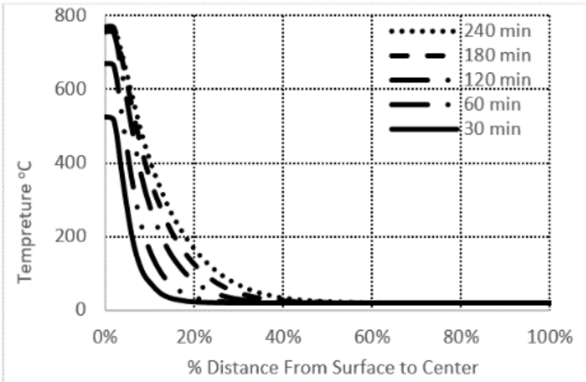


**Figure 38.** Temp. Dist. Through CFST Φ 1600 mm t 20 mm

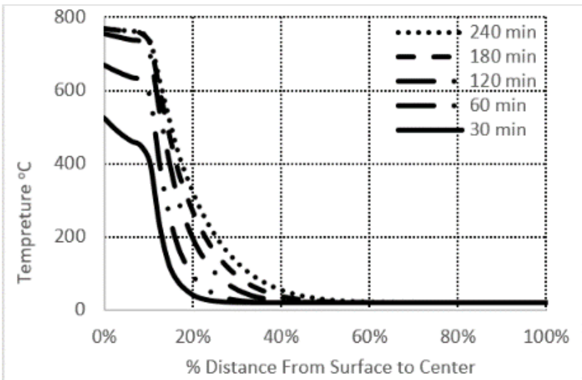


**Figure 39.** Temp. Dist. Through CFST Φ 1600 mm t 80 mm

It could be noticed that slim columns, of order 100 mm, reached a uniform temperature distribution after four hours of fire exposure.

It could also be seen that there is a significant difference in temperature distribution within the steel tube than the concrete core, due to difference in thermal conductivity, specific heat, and exposure condition of the two different materials. This difference is reflected in structural performance, where steel degrades rapidly than concrete. The case of very thick column (Φ1600) did not show any rise in temperature within most of the concrete section, and consequently this will decrease its vulnerability to fire load.

Structural response of CFST to fire load in presence of a superimposed load has been studied extensively to clarify the role of various structural parameters in determining column's fire endurance. Since the presence of steel tube surrounding concrete ensures a high level of confinement; buckling has become the most relevant and critical failure pattern that could take place in CFST. An overall buckling module has been implemented, taking into consideration both non-uniform temperature distribution, thermally induced stresses, and material degradation at elevated temperature. Finite element models outputs in the form of fire endurance have been presented in a number of figures, separating interfered parameters to enable reaching reliable conclusions.

Effect of slenderness ratio has been studied by changing length of column for the same diameter. Four models of thickness 600mm and 1600mm have been studied with lengths 40000mm and 8000mm, as shown in figures (40) and (41).

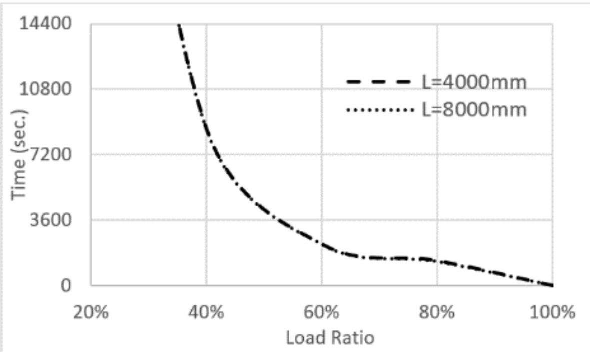


**Figure 40.** Fire Endurance for Φ600mm, t10mm

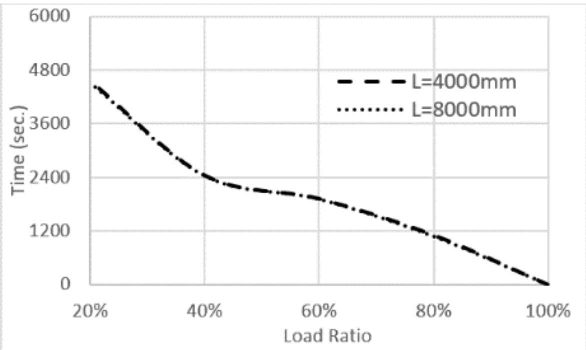


**Figure 41.** Fire Endurance for Φ1600mm, t80mm

It could be noticed that column stiffness is not a parameter for fire endurance relative to load ratio. This could be attributed to that thermally induced stresses are function of temperature rise within column's section in addition to material thermal expansion. the first parameter has been neutralized by comparing columns of the same cross section. While the second parameter generates stresses proportional to thermal strain, which is a percentage of the column's length, independently of length value. This results in a fire endurance, independent of column's length.

Effect of section factor (fire exposed surface / total volume) has been studied for two different cases. The first case changed column diameter, considering the same steel ratio. While the second case changed column diameter, considering the same tube thickness. The first case is presented in figures (42) up to (46), introducing effect of changing column diameter on fire endurance, for ratios of (Φ/t) ranging from (5) up to (80).

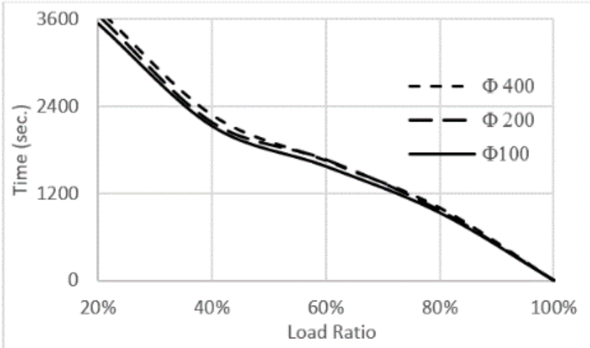


**Figure 42.** Fire Endurance for Φ / t = 5

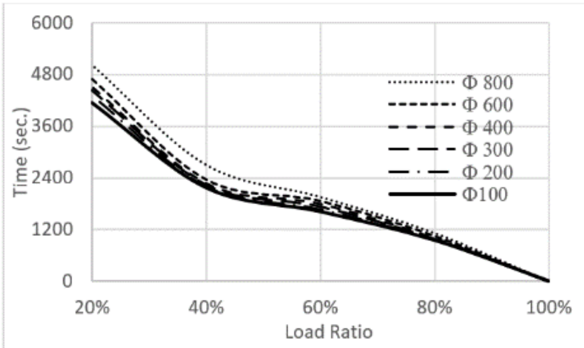


**Figure 43.** Fire Endurance for Φ / t = 10

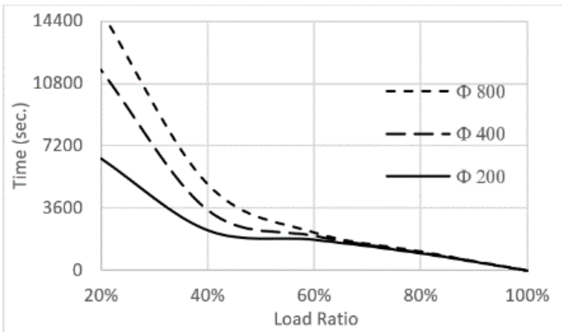


**Figure 44.** Fire Endurance for Φ / t = 20

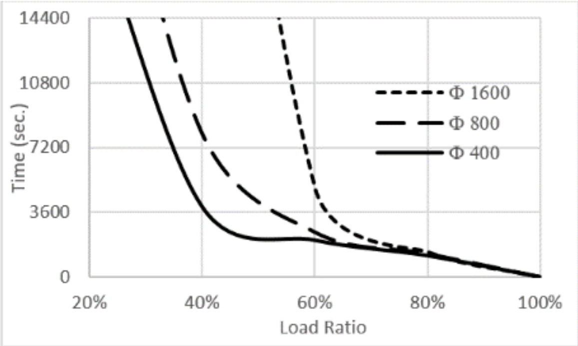


**Figure 45.** Fire Endurance for Φ / t = 40

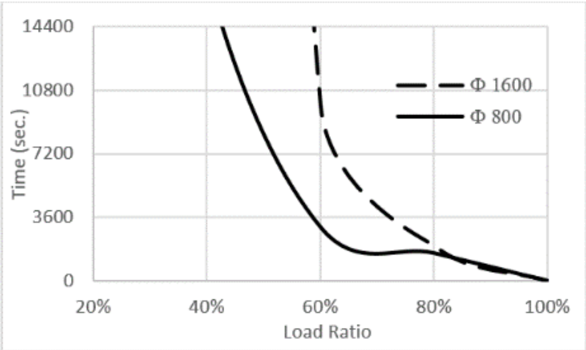


**Figure 46.** Fire Endurance for Φ / t = 80

It could be seen that the increase in the ratio (Φ/t) results in a higher fire endurance. This could be attributed to that the more the ratio (Φ/t), the more the contribution of concrete in column load capacity, than steel. And since concrete suffers less degradation in its structural properties, due to its higher thermal capacity and being away of direct fire exposure, than steel; then fire endurance in columns with high ratio (Φ/t) is expected to be higher than lower ones.

The rate of increase in fire endurance by the decrease in load ratio increases significantly for low load ratios. This increase is higher for high (Φ/t) ratios than low ones, due to the lower vulnerability of concrete than steel to fire, as discussed before.

It could be noticed that there is no significant effect for the change in CFST diameter, for high load ratios. This could be attribute to the high increase in temperature in the beginning of fire load application. This result in an early increase in CFST temperature, and consequently sudden degradation in structural properties, affecting columns of various diameters. That degradation in column's structural properties results in early failure at high load ratio, where columns are highly vulnerable to any material degradation.

Section factor role has also been investigated by studying different column diameters for the same tube thickness, as shown in figures (47 and 48).

It could be seen that each section factor results in a high fire endurance at a specific load ratio, at which total degradation does not reach the level that causes failure. It could also be seen that section factors, exceeding 0.01mm$^{-1}$ (Φ 400 and less) suffered failure within the first four hours of fire load at all load ratios for tube thickness of 20 mm, while only section factors, exceeding 0.02mm$^{-1}$ (Φ 200 and less) behaved the same for tube thickness of 10 mm. Moreover, fire endurance appeared to increase by the decrease in tube thickness, as a result of concrete higher thermal capacity and less structural degradation. Moreover, that rate of increase is higher for thick than slim columns. It could be noticed that in case of load ratios exceeding 80% column diameter is insignificant, as all models suffered failure within the first 20 minutes, as a minor degradation is enough to result in failure.

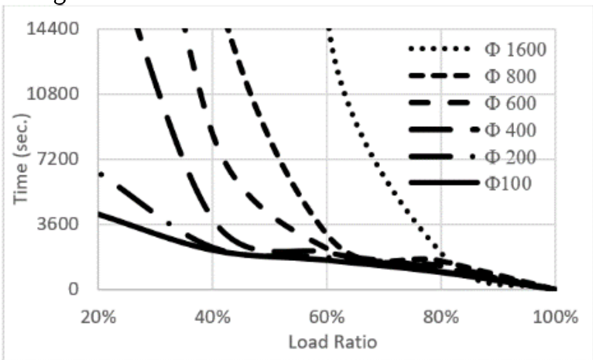


**Figure 47.** Fire Endurance for various diameters at t= 100 mm

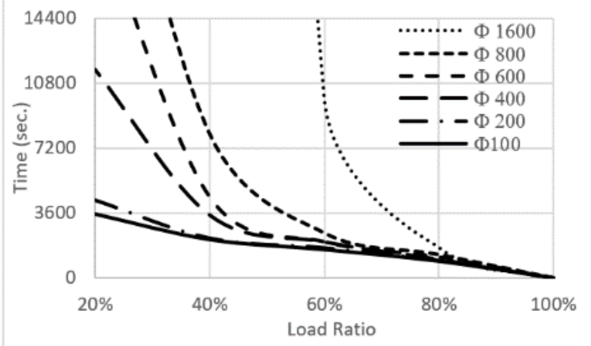


**Figure 48.** Fire Endurance for various diameters at t= 200 mm

The effect of single sided fire load has been investigated by applying fire load to half the tube perimeter along the full column height. Single sided fire loading arises as an unsymmetrical case of loading, enhancing failure in a specific direction. Figure (49) shows full and half load fire endurance for columns of diameters (100mm), (200mm), and (300mm); with ratio (Φ/t=10).

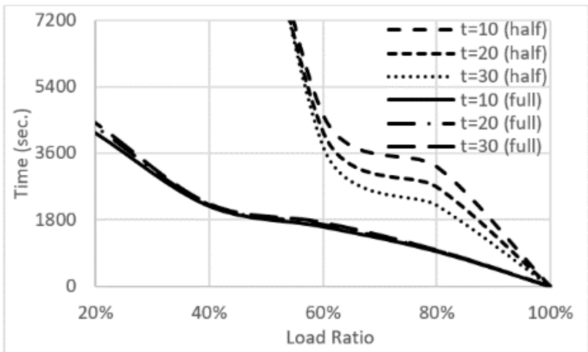


**Figure 49.** Fire Endurance for Φ 100, 200, and 300 mm; full and half fire load (Φ/t =10)

It could be noticed that single sided fire loading has shown a less critical fire endurance. This could be attributed to the limited degradation in column's structural properties, resulting from single sided heating- up.

It could be seen that fire endurance in case of half perimeter thermal loads rises extensively in case of load ratio below 60%. While high load ratio, exceeding 80%, results in an enhanced failure.

It could be noticed that, even all CFST, presented in figure (49) have the same steel ratio; but columns with thicker steel tubes sustained less fire endurance than other thin tubes. This could be attributed to the high thermal conductivity of steel that enabled thicker tubes to transmit heat flux around the column, raising concrete temperature in the rear fire side.

Steel ratio has been studied for three column thicknesses (Φ 200 mm, Φ 400 mm, & Φ 600 mm). The role of tube thickness appeared to be a significant parameter, in conjunction with overall column diameter, as shown in figures (50) up to (52).

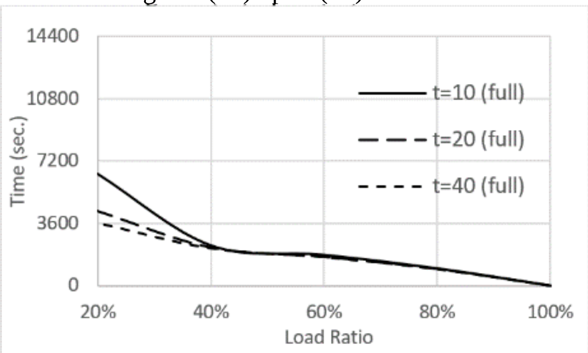


**Figure 50.** Fire Endurance for various tube thickness [Φ200]

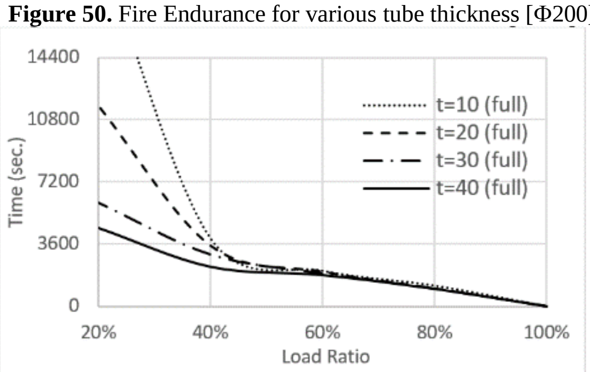


**Figure 51.** Fire Endurance for various tube thickness [Φ400]

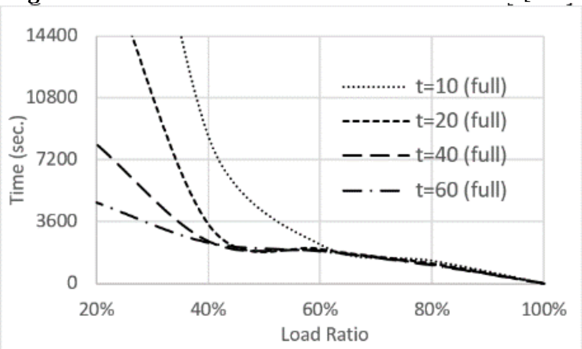


**Figure 52.** Fire Endurance for various tube thickness [Φ600]

Studying figures (50) up to (52), showed that the increase in steel ratio results in a decrease in fire endurance, which could be attributed to the increased portion of load carried by steel that degrades rapidly in case of fire, in addition it is in a direct exposure to fire.

Effects of tube thickness appeared clearly in columns with large diameter than small ones due to the high fire endurance of the large columns, resulting from their delayed heating up, as shown in temperature distribution figures; previously presented in thermal analysis section.

## 4. Conclusions

Analysis of research outputs have arisen valuable conclusions on both thermal and structural aspects. A reliable model has been prepared to study thermo-structural behavior of CFST in fire condition. The model could reveal heating-up patterns, for both full and half thermal loads. Moreover, temperature distribution figures have been prepared for a number of common CFST diameters with a variety of associated tube thicknesses. Temperature distribution curves could be used as design aids. Structural analysis showed that column slenderness is insignificant towards fire endurance, for a specific load ratio. Columns of thicker tube thickness showed less fire endurance than thin tube thickness. Finally, the role of section factor in fire endurance has also been studied, where it could be concluded that columns of diameters 400mm and more showed fire endurance of more than 30 minutes, for a load ratio less than or equal 40 % (common design ratio).

## 5. References

**1.** João Rodrigues & Luís Laím " Behavior of Concrete-Filled Circular, Square, Rectangular, and Elliptical Hollow Columns Subjected to Fire", ASCE structural journal, Vol. 144, Issue 6, June 2018. DOI: 10.1061/(ASCE)ST.1943-541X.0002035

**2.** Tiziano Perea et al " Full-Scale Tests of Slender Concrete-Filled Tubes: Axial Behavior", ASCE structural journal, Vol. 139, Issue 7, July 2013, DOI: 10.1061/(ASCE)ST.1943541X.0000784.

**3.** Venkatish Kodur, Mahmoud Deaikat, and Rustin Fike "High temperature properties of steel for fire resistance modelling of structures", ASCE journal of materials for civil engineering, Vol. 22, Issue 5, May 2010, DOI: 10.1061/(ASCE)MT.19435533.0000041

**4.** J Khalaf, Z Huang, & Mizi Fan "A Study about the effect of bond between steel reinforcement and concrete under fire conditions", 11th International Conference on Developments in E Systems Engineering, June 2018. DOI 10.1109/DeSE.2018.00031

**5.** Lin-Hai Han, et al " Behavior of Concrete-Encased CFST Members under Axial Tension", ASCE structural journal, Vol. 142, Issue 2, February 2016. DOI: 10.1061/(ASCE)ST.1943-541X.0001422.

**6.** R. Imani, G. Mosqueda, M. Bruneau, "Finite Element Simulation of Concrete-Filled Double-Skin Tube Columns Subjected to Post-earthquake Fires", ASCE structural journal, Vol. 141, Issue 12, December 2015, DOI: 10.1061/(ASCE)ST.1943-541X.0001301

**7.** Euro code 4 Part 1-2 –October 2001,"Design of Composite Structures-Part 1-2: General rules-Structural fire design ".

**8.** S. Delepine et al" Compared performances of Rayleigh Raman and Brillouin distributed temperature measurements during concrete container fire test ", 25th international on optical fibers sensors, May 2017, DOI: 10.1117/12.2263449

**9.** Zhehan Ma, Yansheng Song, Li Sun "DESIGN FOR FIRE RESISTANCE OF FRP CONCRETE STRUCTURES BASED ON NUMERICAL MODELS", Sixth International Conference on Intelligent Systems Design and Engineering Applications, June 2015, DOI 10.1109/ISDEA.2015.9

**10.** You-Fu Yang et al" Experimental Study and Numerical Analysis of CFSST Columns Subjected to Lateral Cyclic Loading", ASCE structural journal, Vol. 144, Issue 12, December 2018. DOI: 10.1061/(ASCE) ST.1943-541X.0002225

**11.** Rodrigues, Laim and Korzen "Fire Behaviour of Circular Concrete Columns with Restrained Thermal Elongation", Journal of advanced Concrete Technology Vol. 12, Issue 9, September 2014, DOI: 10.3151/jact.12.289

**12.** Tao Z., and Ghannam M. "Heat transfer in concrete-filled carbon and stainless steel tubes exposed to fire". Fire Safety Journal; 61:1-11, 2013, DOI: 10.1016/j.firesaf.2013.07.004

**13.** Ghannam M., Tao Z., and Song T.Y. "Fire resistance tests of concrete filled stainless steel tubular columns", Proceedings of the Composite Construction VII Conference, Queensland, Australia. 2013

**14.** Lin-Hai Han, Tian-Yi Song, Kan Zhou3, and Zhi-Qiang Cui, "Fire Performance of CFST Triple-Limb Laced Columns", ASCE structural journal, Vol. 144, Issue 9, September 2018. DOI: 10.1061/(ASCE)ST.1943541X.0002168

**15.** Po-Chien Hsiao, K. Kazuhiro Hayashi, Ryousuke Nishi, Xu-Chuan Lin, and Masayoshi Nakashima, " Investigation of Concrete-Filled Double-Skin Steel Tubular Columns with Ultrahigh-Strength Steel ", ASCE structural journal, Vol. 141, Issue 7, June 2015. DOI: 10.1061/(ASCE)ST.1943-541X.0001126

**16.** Martin Neuenschwander, Markus Knobloch, and Mario Fontana, " ISO Standard Fire Tests of Concrete-Filled Steel Tube Columns with Solid Steel Core ", ASCE structural journal, Vol. 143, Issue 4, April 2017. DOI: 10.1061/(ASCE)ST.1943-541X.0001695.

**17.** Xiao-ying Zhang, Chun-cheng Gong, " Numerical Simulation of 3-D Temperature in Reinforced Concrete Structure under Fire ", IEEE Journal, April 2009

**18.** Maurice Guerrieri, and Sam Fragomeni, " Mechanisms of Spalling of Concrete Panels of Different Geometry in Hydrocarbon Fire", ASCE structural journal, Vol. 142, Issue 12, December 2016. DOI: 10.1061/(ASCE)MT.1943-5533.0001680